Proceedings of ASME Turbo Expo 2011
GT2011
June 6-10, 2011, Vancouver, British Columbia, Canada

GT2011-45243

AN AERODYNAMIC DESIGN METHODOLOGY FOR LOW PRESSURE AXIAL FANS WITH INTEGRATED AIRFOIL POLAR PREDICTION

Thomas H. Carolus
University of Siegen
Department of Fluid- and Thermodynamics,
57068 Siegen, Germany

Ralf Starzmann
University of Siegen
Department of Fluid- and Thermodynamics,
57068 Siegen, Germany

ABSTRACT

A common blade design methodology for low solidity fan rotors is based on blade element theory combined with empirical airfoil lift and drag data. Often the required airfoil characteristics have to be estimated from existing wind tunnel data, roughly estimating the effects of Reynolds number and airfoil modifications such as trailing edge thickening. This contribution presents an extension of that methodology: Polar curves are computed during the fan design procedure and applied to each blade element. Reynolds and even Mach number as well as all geometrical features of the airfoil are fully taken into account. For that the public domain code XFOIL for analysis of subsonic isolated airfoils by Drela and Youngren has been integrated in an existing blade design code. The paper summarizes blade element theory and points out the interface where XFOIL data enter. A case study demonstrates how the airfoil specification affects the fan blade design. Two fan rotors for the same duty point but with NACA 4512 and FX60-126 airfoil blades are compared. Moreover, the effect of trailing edge bluntness on the blade shape is investigated.

NOMENCLATURE

c	flow velocity in the stationary frame of reference
c_L	lift coefficient
c_D	drag coefficient
d	diameter
D	drag
f	camber
F	force
L	lift
l	chord length
n	speed
r	radius
t	blade spacing
th	thickness
u	circumferential velocity of rotor
$\dot{V}$	volume flow rate
w	flow velocity in the rotating frame of reference
y	distance from wall
z	number of blades
α	angle of attack
β	angle between w and rotor plane
γ	stagger angle
δ	specific rotor diameter
Δp_{tt}	total to total pressure rise
ε	drag to lift ratio
η	efficiency
λ	blade sweep angle
μ	lift reduction factor due to sweep
ρ	fluid density
σ	specific speed (in introduction), solidity

INTRODUCTION

Low pressure axial fans are required e.g. in engine cooling units for cars, trucks and locomotives, in forced-draft cooling towers and in heating, ventilating and air conditioning systems. They need to be designed for large volume flow rates at a relatively small pressure rise. In terms of non-dimensional 'specific speed' and 'specific rotor diameter'

$$\sigma = \frac{n}{\left(2\pi^2\right)^{-1/4} \left(\Delta p_{tt}/\rho\right)^{3/4} \dot{V}^{-1/2}} \tag{1}$$

$$\delta = \frac{D}{\left(8/\pi^2\right)^{1/4} \left(\Delta p_{tt}/\rho\right)^{-1/4} \dot{V}^{1/2}} \tag{2}$$

they cover the operational range in the low right corner in the Cordier-diagram of turbomachinery, Fig. 1. Note that the index "*opt*" in Fig. 1 refers to the design point, i.e. the operating point with maximum efficiency.

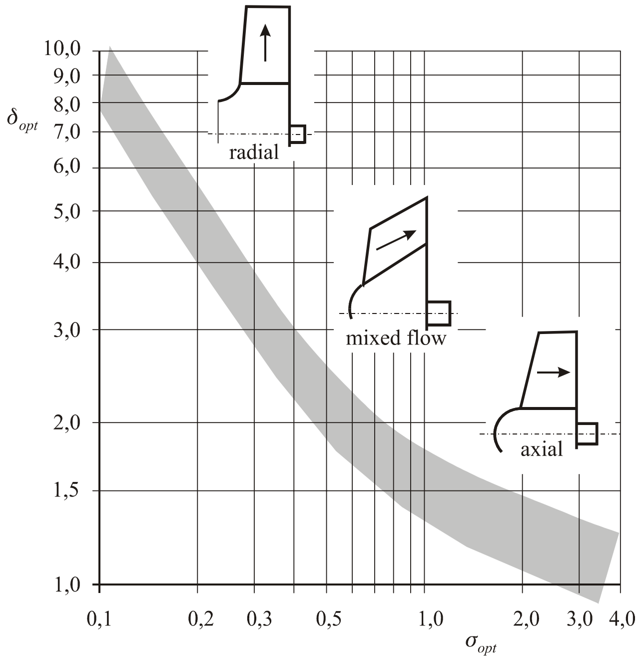

Fig. 1. Specific rotor diameter vs. specific speed of high performance fans; after Cordier, see [1]

The rotors of those fans require low solidity blading, i.e. the circumferential blade spacing is quite large. Usually two-dimensional cascade wind tunnel data are available for high to medium solidity cascades - e.g. Lieblein's data cover cascade solidities down to 0.4 [2]. In low solidity cascades each blade may be considered acting like an isolated airfoil with minor aerodynamic interaction of adjacent blades. Hence, a well-known blade design methodology combines momentum theory with lift and drag characteristics of isolated airfoil sections, also called blade element (BE) theory. A precursory method applied to axial fan design probably origins from Keller, 1934 [3]; Pfleiderer [4] traces it back to as early as 1922, when Bauersfeld used it for the design of propellers and water turbines; the classical analysis of wind turbines by Betz and Glauert is based on this method as well, see Manwell et al. [5].

Among others the success of this design method relies on the quality of airfoil section lift and - to a minor degree - drag data. Up to now in the industrial fan community these data are either estimated or taken from catalogues based on wind tunnel tests. In general this is not satisfactory. For instance, designers of small fans often face the problem of low Reynolds numbers. Depending on the inlet turbulence there is a Reynolds number below which airfoil section and hence fan performance begins to deteriorate, Wallis [6]. Only in rare cases airfoil section data for the Reynolds number in question are available. Another example: The effects of geometrical modifications such as trailing edge thickening or airfoil blending (because of manufacturing and blade strength specifications) almost never are taken into account due to lack of appropriate airfoil data. Finally: Although sound generating mechanisms in axial fans are numerous, a more recent focus is on low-noise airfoils. Evidently there are airfoils with more favorable aero-acoustic characteristics than others, see the experimental findings by Oerlemanns [7], Winkler and Carolus [8]. These all leads to the conclusion that an improved low pressure fan design method needs to incorporate the accurate aerodynamic properties of arbitrary airfoils under a large range of operating conditions. Polar curves at given Reynolds and Mach number need to be computed and applied to the each blade element. Hence, the objective of this work is to fully integrate an isolated airfoil analysis into the classical blade element fan design procedure. For that we select the state-of-the-art public domain airfoil analysis code XFOIL and incorporate it in an in-house Matlab™ based fan design code.

The first sections of this paper summarize the blade element method and points out where the airfoil analysis enters. In the final section we present a case study which demonstrates how details of the airfoil geometry affect the design result.

Note that this paper deals with the design of a fan for a specified design point only. The prediction of a complete characteristic curve is often done in a second step employing a computational fluid dynamics (CFD-) method.

BLADE DESIGN METHODOLOGY

The design method for axial fans is made up of the following steps:

- Preliminary setting of rotor and hub diameter as well as rotor speed; often assisted by empirical correlations such as the Cordier-diagram of turbomachinery, Fig. 1
- Determination of the blade design flow rate and total pressure rise
- Segmentation of the bladed annulus in small blade elements (BEs)
- Choice of spanwise load distribution and computation of velocity triangles required to obtain the blade total pressure rise at design flow rate
- Choice of airfoil, blade sweep and computation of cascade solidity

The main focus of this paper aims on the very last step. For completeness, however, the first steps are summarized as well.

Blade design parameters

Starting point is the fan's global design volume flow rate and total to total pressure rise. Due to volumetric and hydraulic losses the blades need to be designed for:

$$\dot{V}_{bl} = \frac{\dot{V}}{\eta_{vol}} \tag{3}$$

$$\Delta p_{bl} = \frac{\Delta p_{tt}}{\eta_{hyd}} \tag{4}$$

The volumetric and hydraulic efficiency have to be estimated prior to the design process and can be confirmed by a subsequent CFD-analysis of the preliminary design outcome. Note that the fluid density ρ is assumed to be constant for this type of machines, hence it is sufficient to deal with the volume rather mass flow rate.

Annulus Segmentation and Velocity Triangles

In a second step we segment the bladed annulus into small blade elements (BEs), for which the rotor and flow velocities are assumed to be independent of radius, Fig. 2. δr either can be constant for each BE or selected such that, for instance, the BEs' through-flow cross sections are kept constant along the radius. The volume flow rate through a BE is $\delta \dot{V}_{BE}$. Then the axial (meridional) flow velocity can be calculated as

$$c_{m1} = c_{m2} = c_m = \frac{\delta \dot{V}_{BE}}{2\pi r \delta r} \tag{5}$$

Euler's equation of turbomachinery

$$\Delta p_{BE} = \rho u\left(c_{u2} - c_{u1}\right) = \rho 2\pi n\left(c_{u2} - c_{u1}\right) \tag{6}$$

yields the tangential components c_{u2} of the flow velocity the fluid has to leave the BE with in the stationary frame of reference. The standard case is the blade design for a rotor without inlet guide vanes, i.e. $c_{u1} = 0$.

Now the designer has to specify the radial loading distributions $rc_{u2}(r)$. A generalization of Horlock's ansatz [9] is

$$rc_{u2} = \sum_{k=0}^{K} a_k r^k \tag{7}$$

with a_k being constants. Application of the well-known (simple) radial equilibrium condition for the outflow

$$\eta_{hyd} 2\pi n \frac{d\left(rc_{u2}\right)}{dr} = \frac{c_{u2}}{r}\frac{d\left(rc_{u2}\right)}{dr} + c_{m2}\frac{dc_{m2}}{dr} \tag{8}$$

(see e.g. [10]) yields the associated radial distribution of the meridional flow velocity $c_{m2}(r)$. The constants a_k must be set such that the overall targets

$$\dot{V}_{bl} = \int_A d\dot{V} = \int_A c_{m2}(r) dA = \int_{r_i}^{r_o} c_{m2}(r) 2\pi r dr \tag{9}$$

$$\dot{V}_{bl} \Delta p_{bl} = \int_A \frac{\Delta p_{BE}}{\rho} d\dot{m} = \int_{r_i}^{r_o} r 2\pi n c_{u2}(r) \rho c_{m2}(r) 2\pi r dr \tag{10}$$

are achieved. This requires iteration. Note that the special case of the so called free vortex design is $K = 0$, i.e. $rc_{u2}(r) = a_0 =$ const. For that eq. (8) yields $c_{m2}(r) =$ const. as well. The free vortex design usually requires highly twisted blades and a maximum loading of the critical hub BE. This can be avoided by shifting load away from the hub towards BEs in the middle or outer region of the blade. $K = 1$ or 2 allow such loading distribution. The results of this step are the velocity triangles as shown in Fig. 3.

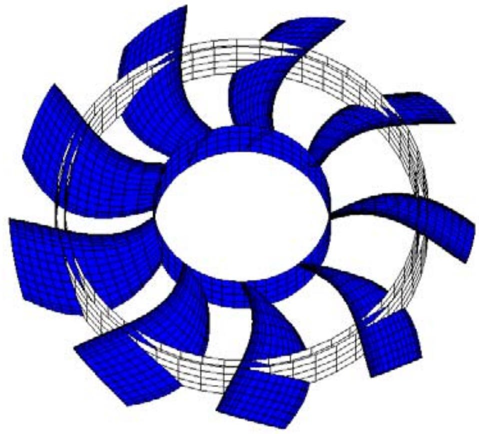

Fig. 2. Blade element (BE) for segmentation of the bladed annulus; each BE has a radial thickness δr

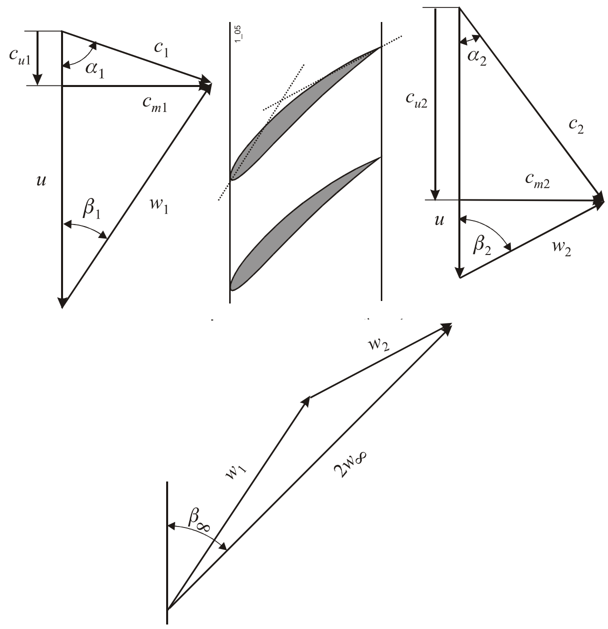

Fig. 3. Velocity triangles at BE (schematically)

Cascade Solidity

Central idea is to derive the tangential force on a BE (i) from the fan's design point via momentum conservation and (ii) from lift and drag of the isolated airfoil section in the cascade. Equating yields the solidity of the BE for given airfoil lift and drag. Conservation of momentum applied to the BE in Fig. 4 (top) yields a tangential force

$$\delta F_u = (c_{u2} - c_{u1})\delta \dot{m} \tag{11}$$

Inserting $\delta \dot{m} = \rho c_m t \delta r$ as mass flow rate through the BE and Euler's equation (6) eventually yields

$$\delta F_u = c_m \frac{\Delta p_{BE}}{u} t \delta r \tag{12}$$

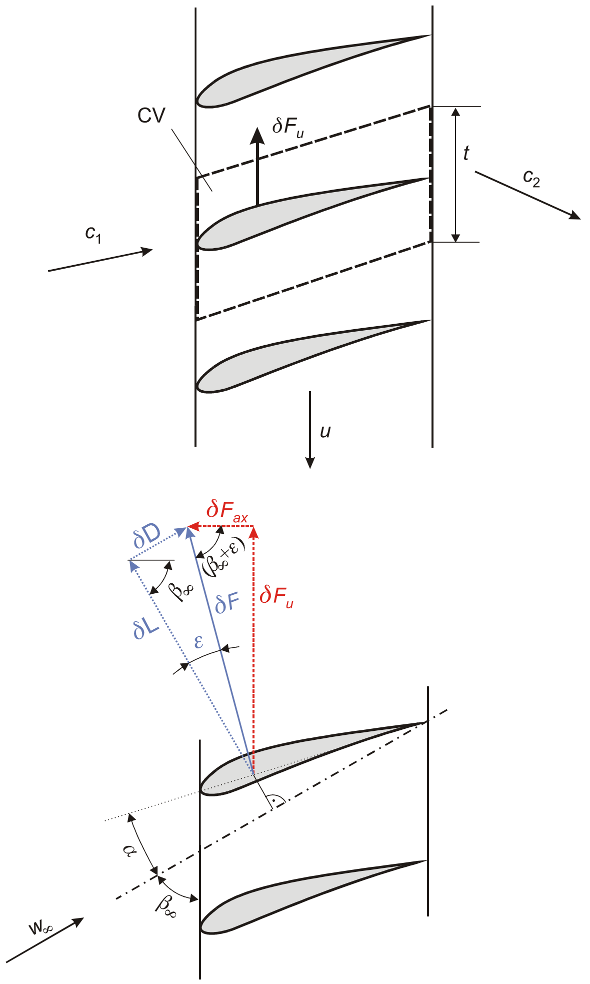

Fig. 4. BE: Velocities and tangential force

On the other hand the tangential force can also be obtained from the force δF on an isolated airfoil element in a flow with velocity w_∞, Fig. 4 (bottom),

$$\delta F_u = \sin(\beta_\infty + \varepsilon)\delta F \tag{13}$$

w_∞ is the vector mean of the flow velocities the fluid enters and leaves the BE with in the rotating frame of reference $\left|\frac{1}{2}(\vec{w}_1 + \vec{w}_2)\right|$, i.e.

$$w_\infty = \frac{1}{2}\sqrt{\left(u + \sqrt{w_2^{\,2} - c_m^{\,2}}\right)^2 + 4c_m^{\,2}} \tag{14}$$

The flow angle with respect to the cascade inlet plane is

$$\beta_\infty = \arctan\left(\frac{2c_m}{u + \sqrt{w_2^{\,2} - c_m^{\,2}}}\right) \tag{15}$$

Since the drag is usually much smaller than the lift, $\delta F \approx \delta L$. With

$$\delta A = c_L \rho \frac{w_\infty^2}{2} l \delta r \tag{16}$$

one obtains

$$\delta F_u = \sin(\beta_\infty + \varepsilon) c_L \rho \frac{w_\infty^2}{2} l \delta r \tag{17}$$

c_L is the lift coefficient, ε the drag to lift ratio of the airfoil section.

Equating eqs. (12) and (17) eventually yields the key equation for the design of low solidity blade cascades

$$\frac{l}{t}(\equiv \sigma) = \frac{\overbrace{\Delta p_{BE}}^{\text{design pressure rise}}}{\underbrace{\frac{\rho}{2} w_\infty u}_{\text{fluid property and velocities}} \underbrace{c_L \left(1 + \frac{\varepsilon}{\tan \beta_\infty}\right)}_{\text{airfoil properties}}} \tag{18}$$

It connects the required cascade parameter 'solidity' with the chosen airfoil section parameters 'lift' and 'drag' (via the drag to lift ratio), and the fan global design target 'pressure rise' and 'volume flow rate' via the velocity triangles.

The lift of the airfoil section is affected by a possible sweep which is often desirable for acoustic reasons. Fig. 5 shows a front view of a blade with negative sweep angle λ in the hub and positive in the tip region. As a rule of thumb: acoustic benefits require sweep angles larger than 40°. To avoid any additional dihedral (on top of the small one due to blade twisting), we only consider BE sweep in a plane parallel to the local mean flow angle β_∞. Two effects are due to sweep: (i) The lift is reduced by a factor $\cos\lambda$. (ii) A swept back wing approaching a wall produces less lift than an infinite wing, a swept forward more; this has been analysed by Küchemann and Weber [11] and used for fan design slightly modified by Beiler [12, 13] (see also Clemen an Stark [14]). The wall correction e is a function of the ratio of wall distances y over chord length l and affects mainly the wing sections within a distance of one chord length from the wall. Combined, the effective lift of the swept blade with adjacent walls becomes a fraction of the straight blade without wall effect

$$\mu \equiv \frac{c_L|_{\text{swept,with endwall}}}{c_{L,\infty}} = (\cos\lambda)^{\tau} e(y/l) \tag{19}$$

Beiler [12, 13] found a better agreement with fan measurements when τ was set to 0.62 rather 1 as the original theory suggests. Fig. 6 shows this lift correction function for some positive and negative sweep angles. The lift correction function is used to compensate for sweep and wall effects by either correcting σ or superimposing a twist correction to each BE.

The procedure is now as follows:

- Compute right hand side of eq. (18) and obtain the required solidity σ; c_L and ε origin from the designer's specification of an airfoil and angle of attack α.
- Select number of blades z, compute circumferential BE spacing $t = 2\pi r/z$ and determine required chord length l.
- Compute stagger angle $\gamma = \beta_\infty + \alpha$ (Fig. 7).

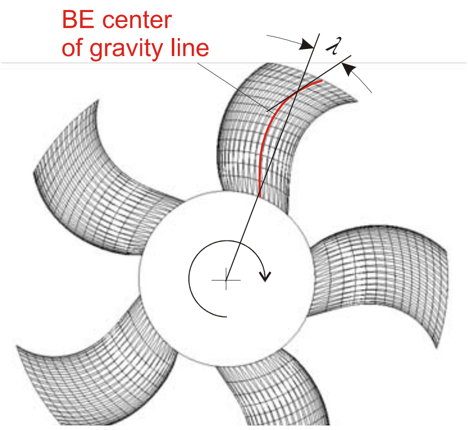

Fig. 5. Swept bladed fan rotor; actually, the sweep angle λ is defined in a plane parallel to the local mean flow angle β_∞

Occasionally we apply two further corrections. To take into account that the airfoil operates in a deflected flow (from β_1 to β_2) rather in a free stream of e.g. a large wind tunnel, we add this 'camber'

$$\left.\frac{f}{l}\right|_d = \frac{1}{2} tan\left(\frac{\beta_2 - \beta_1}{4}\right) \tag{20}$$

to the camber of the original airfoil $\left.\frac{f}{l}\right|_\infty$ and obtain a modified airfoil camber

$$\frac{f}{l} = \left.\frac{f}{l}\right|_\infty + \left.\frac{f}{l}\right|_d \tag{21}$$

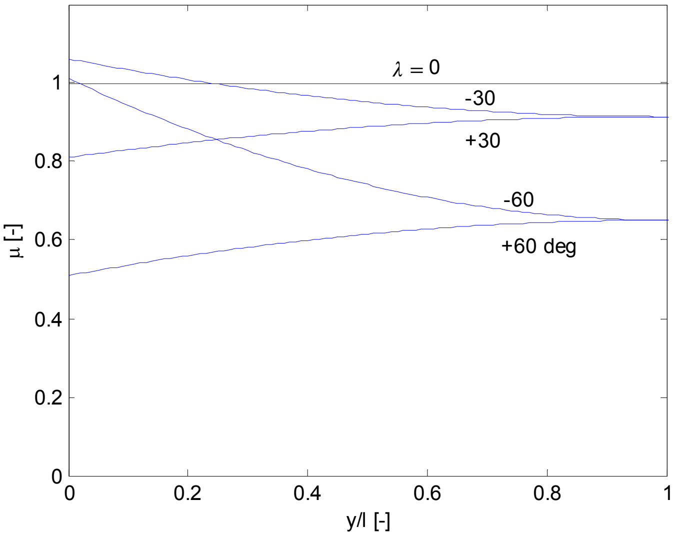

Fig. 6. Lift correction as a function of the distance from the wall (casing or hub) for various sweep angles λ

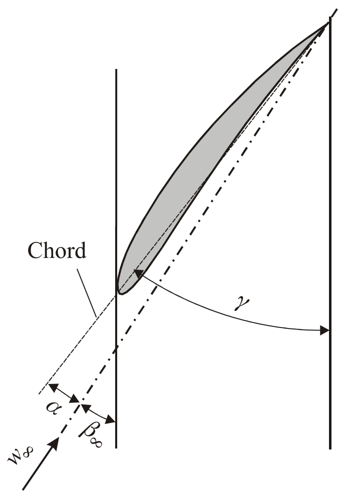

Fig. 7. Definition of stagger angle γ

On top of that one can correct for the blockage of the bladed annulus by the airfoils with their maximum thickness d. Marcinowski [15] suggests a semi-empirical correction of the angle of attack as

$$\alpha_d = 0.5\left\{\gamma - \arctan\left[\tan\gamma - \left(\frac{d}{t\cos\gamma}\right)\right]\right\} \tag{22}$$

α_d has to be computed iteratively. Eventually the stagger angle becomes

$$\gamma = \beta_\infty + \alpha + \alpha_d \tag{23}$$

XFOIL

As pointed out c_L and ε origin from the designer's choice of an airfoil and the angle of attack α. Here XFOIL 6.9 is integrated to assist in calculating the airfoil performance in terms of c_L and ε polars and to identify the optimal angle of attack. XFOIL has been written by Drela and Youngren for design and analysis of subsonic isolated airfoils, see e.g. [16]. Here we use the viscous analysis option of airfoils, allowing the accurate prediction of airfoil polars as a function of Reynolds (and even Mach) number. In fan design the correct Reynolds number rarely is taken into account accurately. Particularly when designing small fans this may cause considerable inaccuracies. Another feature we take advantage of is that arbitrary blunt trailing edges can be incorporated. This is important since manufacturing and handling reasons usually prohibit fan blades with a sharp trailing edge.

The fan design method as described in section 2 is implemented in Matlab™ [17]. Originally XFOIL is an interactive program. Here, however, it is called via a short script of commands within the Matlab code. Among other standard values we set the number of panels to 200, the number of iterations to 500 and the transition criterion Ncrit to 9 (corresponding to the freestream turbulence of an average wind tunnel).

CASE STUDY

As an example we design a fan rotor for a total to total pressure rise of 140 Pa at a volume flow rate 0.7 m^3/s. We select a rotor diameter d_0 = 400 mm, a hub to tip ratio 0.44 and a speed n = 1420 rpm. Two options of airfoils which look similar at a first glance are checked: (i) a 4-digit NACA airfoil 4512 with its maximum camber of 4% at 50% of the chord and a maximum thickness of 12%, (ii) a Wortmann airfoil FX60-126 with its maximum camber of 3.56% at 56.5% of the chord and a maximum thickness of 12.59%. Both airfoils are modified by linearly increasing the thickness from leading to trailing edge such that the trailing edge thickness is 1 mm. Fig. 8 illustrates the two airfoils. Fig. 9 presents the polar curves for the BEs at hub, midspan and tip as obtained by XFOIL. The Reynolds number ranges from 60,000 at hub to 100,000 at tip. These values explain the strong effect of Reynolds number on lift and even more on drag. The angles of attack are already set such that they lie in the low drag to lift ratio region of the airfoil characteristic.

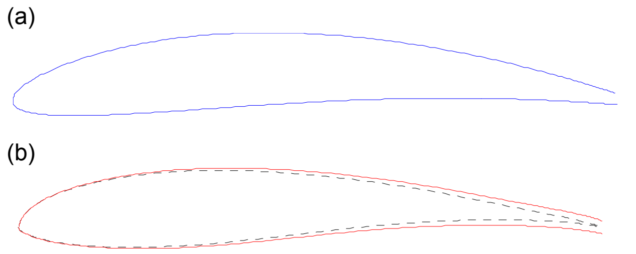

Fig. 8. (a) NACA 4512, (b) FX60-126 (dashed line: original contour, solid line: modified for specified blunt trailing edge) [18, 19]

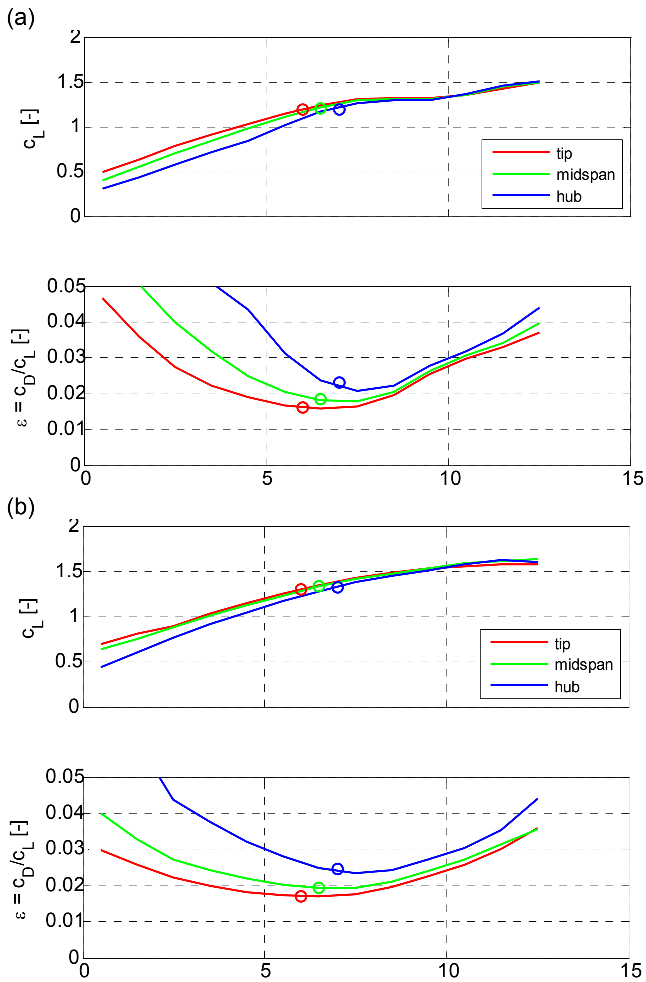

Fig. 9. Computed polar curves and airfoil operating points at hub, midspan and tip BE; (a) NACA 4512, (b) FX60-1120

The polars for the two airfoils are similar but not the same. Given the same angle of attack α FX60-120 yields a slightly larger lift. This leads to blades with a smaller chord length as compared to the NACA airfoil blades, Fig. 10 and Fig. 11.

Also, the FX airfoil has a low drag bucket which extends over a larger α-range as compared to the NACA polar. This may produce a more favorable characteristic curve of the fan with stall shifted to smaller volume flow rates and a flattened efficiency characteristic.

Fig. 12 presents the effect of trailing edge thickness. 2 mm corresponds to a trailing edge thickness to chord ratio of 2.5% at hub and 4% at tip. It is somewhat surprising how large the effect of the trailing edge thickness on the aerodynamic performance is. The prediction shown is based on the degradation of the lift curve with increasing trailing edge thickness; the decrease in hydraulic efficiency is not taken into account.

SUMMARY AND CONCLUSION

A common blade design methodology for low solidity fan rotors which is based on blade element theory was refined by integrating a state-of-the-art isolated airfoil analysis. This allows a more accurate assessment of various airfoil shapes for fan blading, taking into account (i) the true Reynolds (and even Mach) number at each blade section and (ii) geometrical airfoil modifications such as e.g. anthe unavoidable blunt trailing edge.

An essential limitation of the methodology is clearly due to the assumption that each blade acts like an isolated airfoil with negligible aerodynamic interaction of adjacent blades. In general this holds true for low pressure axial fans, at least for the outer blade sections. In some cases, however, this assumption is violated towards the blade root demanding a design method based on medium to high solidity cascade data. Those are available for a few types of airfoils. A further refinement of the method described here could be a hybrid approach with a blending of cascade and isolated airfoil data. This is feasible since the isolated airfoil method presented is able to handle nearly arbitrary airfoils. Another limitation is the convergence of the airfoil analysis code. Here we use XFOIL which is a numerical flow solver. In most cases XFOIL's performance is quite stable but one should at least provide high quality airfoil coordinates.

There is some evidence (not shown here) that a fan designed employing XFOIL within the design process meets the design target more accurately. With the consequence that the number of iterations required obtaining a fan very close to the design target may be reduced considerably. However, CFD-analysis, prototyping and testing still can not be avoided completely.

As for many analytical methods the design is limited to the fan's design point. Ways obtaining a complete performance curves are a CFD-analysis (a RANS method should be sufficient) and/or prototyping and experimental determination of the fan characteristics on a standardized fan test rig.

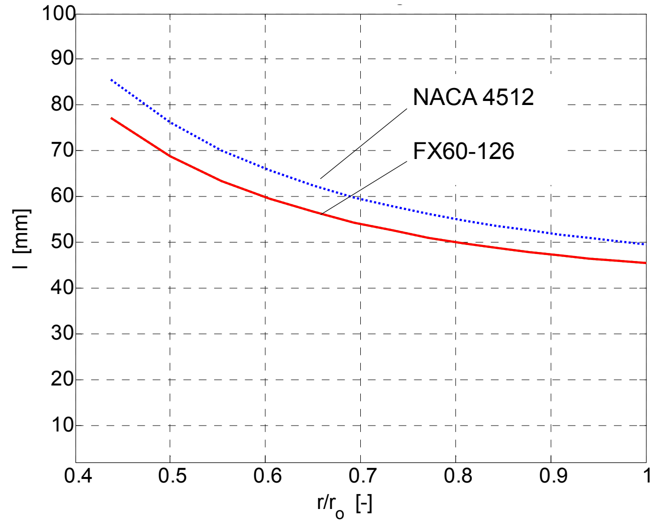

Fig. 10. Effect of airfoil on blade chord required

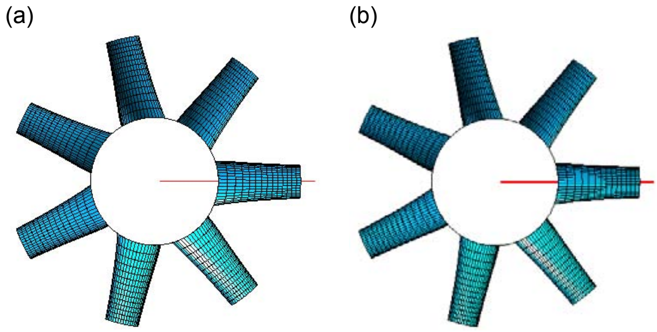

Fig. 11. Seven bladed rotor; (a) with NACA 4512, (b) with FX60-1120 airfoil blades

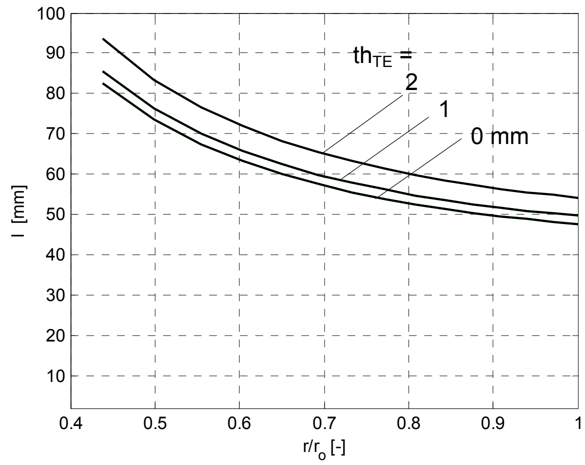

Fig. 12. Effect of trailing edge thickness on blade chord required

REFERENCES

[1] Fister, W.: Fluidenergiemaschinen, Band 1: Physikalische Voraussetzungen, Kenngrößen, Elementarstufen der Strömungs- und Verdrängermaschinen. Springer-Verlag, 1984

[2] Members of the Staff of Lewis Research Center: Aerodynamic design of axial-flow compressors. NASA SP-36, Washington, D.C., 1965

[3] Keller, C.: Axialgebläse vom Standpunkt der Tragflügeltheorie. Dr.-Ing. Diss. ETH Zürich, 1934

[4] Pfleiderer, C.: Die Kreiselpumpen für Flüssigkeiten und Gase. Springer-Verlag, 5. Edition, 1961

[5] Manwell, J.F., McGowan, J.G., Rogers, A.L.: Wind Energy Explained. John Wiley & Sons Ltd., 2009

[6] Wallis, R.A.: Axial Flow Fans and Ducts. John Wiley & Sons Inc., 1983

[7] Oerlemans, S.: Wind Tunnel Aeroacoustic Tests of Six Airfoils for Use on Small Wind Turbines. AAM-2-32237-01, 2004. NRL, Emmeloord, Netherlands

[8] Winkler, J., Carolus, T.: Experimentelle Ermittlung der Auftriebs- und Schallpolaren von Ventilatorschaufelprofilen im Windkanal. Abschlussbericht Nr. F209 102 A der Universität Siegen über das FLT-Vorhaben Nr. L 222, Mai 2009

[9] Horlock, J. H.: Axialkompressoren. Verlag G. Braun, Karlsruhe, 1967

[10] Dixon, S.L.: Fluid Mechanics and Thermodynamics of Turbomachinery, 5. Edition 1998

[11] Küchemann, D., Weber, J.: On the Chordwise Lift at the Centre of Swept Wings. The Aeronautical Quarterly, Vol. 2, pp. 146 155, Aug. 1952

[12] Beiler, B.: Untersuchung der dreidimensionalen Strömung durch Axialventilatoren mit gekrümmten Schaufeln. VDI-Fortschrittberichte Nr. 298, Reihe 7: Strömungstechnik, 1996

[13] Beiler, M., Carolus, T.: Computation and Measurement of the Flow in Axial Flow Fans with Skewed Blades. ASME J. of Turbomachinery, Jan. 1999, Vol. 121

[14] Clemen, D., Stark, U.: Randeffekte in Axialventilatoren mit gesichelten Schaufeln. In: Ventilatoren - Entwicklung - Planung - Betrieb. VDI-Berichte 1591, 2001, pp. 427-422

[15] Marcinowski, H.: Strömungsmaschinen II. Skript zur Vorlesung an der Universität (TH) Karlsruhe, 1975

[16] Drela, M.: XFOIL: An Analysis and Design System for Low Reynolds Number Airfoils, Conference on Low Reynolds Number Airfoil Aerodynamics, University of Notre Dame, June 1989.

[17] Carolus, Th.: Entwurfsprogramm für Niederdruckaxialventilatoren dAX-LP, 1987 - 2010

[18] Abbott, H., von Doenhoff, A. E., Stivers, L. S.: Summary of airfoil data. NACA-Report Nr. 824, 1945

[19] Althaus, D., Wortmann, F.X.: Stuttgarter Profilkatalog I, Vieweg 1981